**M. Jabbari**[*]
Associate Professor

**M. Rezaei**[†]
MSc.

**A. Mojahedin**[‡]
MSc.

**M. R. Eslami**[§]
Professor

# Mechanical Buckling of FG Saturated Porous Rectangular Plate under Temperature Field

*In this study buckling analysis of solid rectangular plate made of porous material in undrained condition is investigated. The mechanical properties of plate are assumed to vary through the thickness direction. Distributing of the pores through the plate thickness are assumed to be the nonlinear nonsymmetric, nonlinear symmetric, and monotonous distribution. The effect of pores and pores distribution on critical buckling load of porous plate are studied. Effect of fluid compressibility on critical buckling load is investigated in the undrained condition. Also, effect of temperature on fluid compressibility for symmetric porous material plate, choosing a linear function, is examined. The results obtained for porous plates are verified with the known data in literature.*

## 1 Introduction

The porous material are made of two elements; one of which is solid (body) and the other element is either liquid or gas which are frequently found in nature. Problems of deflection and buckling of the porous plates have been developed by many authors. The buckling of a fluid-saturated porous slab under axial compression is reported by Biot [1]. He investigated the pore compressibility effect on critical buckling load and expressed that the critical load is proportional to the pore compressibility. He showed lower and upper critical value for a rectangular plate. Buckling of porous beams with varying properties were described by Magnucki and Stasiewicz [2]. They used shear deformation theory to determine the critical load. In this work, the effect of porosity on the strength and buckling load of the beam is investigated too. Magnucki et al. [3] investigated on the bending and buckling of rectangular plate made of foam material which have nonlinear mechanical properties in thickness direction with its material properties being non-symmetric with respect to middle of the plate (porous/nonlinear symmetric distribution plate).

---

[*] Corresponding Author, Associate Professor, Department of Mechanical Engineering, South Tehran Branch, Islamic Azad University, Tehran, Iran Mohsen.jabbari@gmail.com

[†] MSc., Department of Mechanical Engineering, South Tehran Branch, Islamic Azad University, Tehran, Iran Masoud.rezaey@yahoo.com

[‡] MSc., Department of Mechanical Engineering, South Tehran Branch, Islamic Azad University, Tehran, Iran mojahedin.arvin@gmail.com

[§] Professor and Fellow of the Academy of Sciences, Mechanical Engineering, Department of Mechanical Engineering, Amirkabir University of Technology, Tehran, Iran Eslami@aut.ac.ir

They obtained the result for a porous/nonlinear symmetric distribution plate. Magnucka-Blandzi [4] obtained the critical buckling load for rectangular plate made of foam with two layers of perfect material. The core was made of a metal foam with properties varying across the thickness. Jasion et al. [5] derived the analytical, numerical, and experimental critical buckling load for plate and beam made of foam with two layers of perfect material. They obtained global and local buckling-wrinkling of the face sheets of sandwich beams and sandwich circular plates. They also compared values of the critical load obtained by the analytical, numerical (FEM), and experimental methods. Zimmerman [6] studied on the thermoelastic and poroelastic coupling parameters for a linear poroelastic saturated rock. He concluded that poroelastic coupling parameter has a stronger influence compared to the thermoelastic one. Ghassemi et al. [7] showed the effects of temperature gradients on pore pressure and stress distribution by using a non-isothermal poroelasticity theory.

Thereafter, Ghassemi [8] investigated the influence of cooling on pore pressure and stresses distribution by displacement discontinuity method. Jabbari et al. [9,10] considered the poroelastic circular plate under the mechanical and thermal forces with classical plate theory (CPT). They studied the effects of distribution and properties of pores that are saturated by fluid on stability of plate. Jabbari et al. [11,12] considered the stability of sandwich plate with piezoelectric layers and poroelastic core under uniform thermal and electrical field. Also, they achieved their results based on the classical plate theory and first-order theory. They explored the effects of mechanical and thermal properties on stability of poroelastic plate too. Mojahedin et al. [13] studied the buckling of poroelastic plate with piezoelectric layers under electrical, thermal, and mechanical forces. Jabbari et al. [14] considered the buckling of circular porous plate under transverse magnetic field. They explained the effects of mechanical and magnetic properties on stability of porous-magnetic plate. Kumar et al. [15] analysed Interaction due to expanding surface loads in thermoporoelastic medium.

Buckling analysis of porous plates with functional properties have similarities with the FGM plates to some extend. Javaheri et al. [16,17,18] presented the buckling of FGM rectangular plates under in-plane mechanical or thermal loads based on the classical and higher order shear deformation plate theories, respectively. The thermal buckling of simply-supported moderately thick rectangular FGM plates based on the FSDT under different types of temperature fields is investigated by Lanhe [19]. Shariat et al. [20] presented a closed-form solution for the buckling analysis of rectangular thick FGM plates based on the TSDT under mechanical and thermal loads. The buckling analysis of thin FG rectangular plates based on the classical or FSDT under various loads were done by Mohammadi et al. [21,22], respectively.

Bodaghi et al. [23,24] used a Levy-type solution method to investigate the mechanical or thermoelastic buckling of thick FGM rectangular plates based on the TSDT, respectively. Bateni et al. [25] investigated the effect of temperature dependency of material properties on the critical buckling load. In this study, a four-variable refined plate theory is employed to derive the governing equations of equilibrium. A multi-term Galerkin solution is presented to derive the critical buckling loads/temperatures along with the buckled shape of the plate. Behravan Rad et al. [26] investigated three-dimensional magneto-elastic analysis of asymmetric variable thickness porous FGM circular plates with non-uniform tractions and Kerr elastic foundations. A comprehensive review of various analytical and numerical models to predict the bending and buckling under mechanical and thermal loads is done by Swaminathan et al. [27]. Chen et al. [28,29] presented the elastic buckling and static bending solutions based on Timoshenko beam theory also free and forced vibrations of shear deformable functionally graded porous beams.

The aim of the present paper is to derive the general equilibrium and stability equations for rectangular plates made of porous material using the energy method along with the calculus of variations and based on the classical plate theory.

Then, closed form solutions for the rectangular plates subjected to mechanical loading is obtained. The critical buckling load of porous rectangular plates with simply supported boundary condition is obtained. The material property is taken as power law through the thickness of plate. The porous plate is assumed of the form where pores are saturated with fluid. The effect of poroelastic material, such as pores distribution and pores compressibility, on the critical buckling load is investigated. The porous distribution changes mechanical properties through the thickness and variation of fluid properties in porous material changes the compressibility of poroelastic plate. Finally, the results are compared with the buckling loads of rectangular plates obtained in the literature.

## 2 Governing equations

Consider a rectangular plate made of porous materials of thickness $h$, length $a$, and width $b$, referred to the rectangular Cartesian coordinates $(x, y, z)$, as shown in figure (1).

The material properties are assumed to vary through the thickness according to the following power law distribution. The functional relationship between $E$ and $G$ with $z$ for plate is assume as (Magnucki et al. [2] and Magnucka-Blandzi [4])

$$G(z) = G_0 \left[ 1 - e_1 \cos\left( \left(\frac{\pi}{2h}\right)\left(z + \frac{h}{2}\right) \right) \right]$$

$$E(z) = E_0 \left[ 1 - e_1 \cos\left( \left(\frac{\pi}{2h}\right)\left(z + \frac{h}{2}\right) \right) \right] \tag{1}$$

$$e_1 = 1 - \frac{G_1}{G_0} = 1 - \frac{E_1}{E_0}$$

where $e_1$ is the coefficient of plate porosity $0 < e_1 < 1$, $E_1$ and $E_0$ are Young's modulus of elasticity at $z = -h/2$ and $z = h/2$, respectively, $(E_0 \geq E_1)$ and $G_1$ and $G_0$ are the shear modulus at $z = -h/2$ and $z = h/2$, respectively, $(G_0 \geq G_1)$. The relationship between the modulus of elasticity and shear modulus of elasticity for $j = 0$ and 1 is $E_j = 2G_j(1 + v)$ where $v$ is Poisson's ratio, which is assumed to be constant across the plate thickness.

### 2.1 Basic equations

The non-linear strain-displacement relations according to the von-Karman assumption are by Brush and Almroth [30]

$$\varepsilon_{xx} = u_{,x} + \frac{1}{2}(w_{,x})^2$$

$$\varepsilon_{yy} = v_{,y} + \frac{1}{2}(w_{,y})^2 \tag{2}$$

$$\gamma_{xy} = u_{,y} + v_{,x} + w_{,y}w_{,x}$$

**Figure 1** Coordinate system and geometry of rectangular porous material plate

Here, $\varepsilon_{xx}$ and $\varepsilon_{yy}$ are the normal strains and $\gamma_{xy}$ is the shear strain, where $u$, $v$, and $w$ denote the displacement components in the $x$, $y$, and $z$ directions, respectively, and comma indicates the partial derivative with respect to its afterwards. Note that transverse shear strains are zero as $\gamma_{yz} = \gamma_{xz} = 0$ in the Kirchhoff plate theory.

The displacement field for the Kirchhoff plate theory is by Wang et al. [31]

$$
\begin{aligned}
u(x, y, z) &= u_0(x, y) - z w_{0,x} \\
v(x, y, z) &= v_0(x, y) - z w_{0,y} \\
w(x, y, z) &= w_0(x, y)
\end{aligned}
\tag{3}
$$

where $(u_0, v_0, w_0)$ represent the displacement on middle plate surface $(z = 0)$.

The linear poroelasticity theory of the Biot has two features by Detournay and Cheng [32]

1. An increase of pore pressure induces a dilation of pore.

2. Compression of the pore causes a rise of pore pressure.

The stress-strain law for the thermo-poroelasticity is given by Ghassemi [7]

$$
\sigma_{ij} = 2G\varepsilon_{ij} + \lambda_u \varepsilon \delta_{ij} - p\alpha\delta_{ij} - 3K_u \beta'_s T\delta_{ij}
\tag{4}
$$

where

$$
\lambda_u = \frac{2Gv_u}{1 - 2v_u}
$$

$$
v_u = \frac{v + \alpha B(1 - 2v)/3}{1 - \alpha B(1 - 2v)/3}
$$

$$
p = M[\zeta - \alpha\varepsilon + \alpha(\beta_f - \beta''_s)T]
\tag{5}
$$

$$
M = BK_u
$$

$$
K_u = \frac{(2G + 3\lambda)}{3(1 - \alpha B)}
$$

Here, $p$ is pore fluid pressure, $\lambda_u$ is the Lame parameters, $M$ is Biot's modulus, $\zeta$ is variation of fluid volume content, $\nu_u$ is undrained Poisson's ratio $\nu < \nu_u < 0.5$, $B$ is the skempton coefficient, the pore fluid properties is introduced by the skempton coefficient. The values of the undrained Poisson ratio and the Skempton pore pressure coefficients depend on the pore fluid compressibility. Here, $\alpha$ is the Biot coefficient of effective stress $0 < \alpha < 1$. The Biot coefficient $\left(\alpha = 1 - \frac{G(z)}{G_0}\right)$ indicates the effect of porosity on the solid constituents of poroelastic plate and it shows the effect of generated stresses in the pores on the poroelastic material in undrained condition $(\zeta = 0)$ and $(1 - \alpha B)$ is relation between drained bulk modulus and undrained bulk modulus.

The term $\alpha\beta$ is coupling between pore fluid effects and macroscopic deformation Zimmerman [6], $\beta_s'$ is the volumetric thermal expansion coefficient of the bulk solid under constant pore pressure and stress, $\beta_s''$ and $\beta_f$ represent volumetric thermal expansion coefficients of the solid matrix and the pore fluid, respectively. The value of $\beta_s'$ may be considered equal to $\beta_s''$ if the change in temperature is not expected to change the porosity, Ghassemi [7], and $\varepsilon$ is the volumetric strain.

The two dimensional stress-strain law for plane-stress condition in the Cartesian coordinate for the undrained condition $(\zeta = 0)$ is given by

$$\sigma_{xx} = A_1(z)\varepsilon_{xx} + B_1(z)\varepsilon_{yy} - C_1(z)T$$
$$\sigma_{yy} = A_1(z)\varepsilon_{yy} + B_1(z)\varepsilon_{xx} - C_1(z)T \tag{6}$$
$$\sigma_{xy} = G(z)\gamma_{xy}$$

By substituting the third and fourth equations of (5) into Eq. (4), terms $A_1(z), B_1(z), C_1(z)$ and $R_1(z)$ become

$$A_1(z) = 2G(z) + (\lambda_u + M\alpha^2)R(z)$$

$$B_1(z) = (\lambda_u + M\alpha^2)R(z)$$

$$C_1(z) = \left(3K_u\beta_s' + M\alpha^2(\beta_f - \beta_s'')\right)R(z) \tag{7}$$

$$R(z) = 1 - \frac{\lambda_u + M\alpha^2}{2G(z) + \lambda_u + M\alpha^2}$$

*2.2 Strain energy*

The total virtual potential energy of the plate as the sum of total virtual strain energy and virtual potential energy of the applied loads is equal to

$$\delta U = \frac{1}{2} \int_0^a \int_0^b \int_{-h/2}^{h/2} \left(\sigma_{xx}\delta\varepsilon_{xx} + \sigma_{yy}\delta\varepsilon_{yy} + \sigma_{xy}\delta\gamma_{xy}\right)dxdydz \tag{8}$$

Substituting the strain-displacement relations from Eqs. (2) and Eq. (3) into the above equations, and apply the Green-Gauss theorem to relieve the virtual displacements, result in the following three equilibrium equations by Eslami [33]

$$\delta u_0 : N_{xx,x} + N_{xy,y} = 0$$
$$\delta v_0 : N_{xy,x} + N_{yy,y} = 0 \tag{9}$$
$$\delta w_0 : M_{xx,xx} + M_{yy,yy} + 2M_{xy,xy} + N_{xx}w_{0,xx} + N_{yy}w_{0,yy} + 2N_{xy}w_{0,xy} = 0$$

where $N_{ij}$ and $M_{ij}$ are the force and moment resultants defined by

$$\left(N_{ij}, M_{ij}\right) = \int_{-h/2}^{h/2} (1, z)\sigma_{ij}dz \qquad ij = xx, yy, xy \tag{10}$$

## 3 Stability equations

Consider an equilibrium position described by displacement components $u_0^0$, $v_0^0$, and $w_0^0$. Each of these components is perturbed from the primary equilibrium state. An equilibrium state exists adjacent to the primary one, described by the displacement components as by Eslami [33]

$$u_0 \rightarrow u_0^0 + u_0^1$$
$$v_0 \rightarrow v_0^0 + v_0^1 \tag{11}$$
$$w_0 \rightarrow w_0^0 + w_0^1$$

Here, a superscript 1 indicates the magnitude of increment (perturbation). Accordingly, the stress resultants are divided into two terms representing the stable equilibrium and the neighboring state. The stress resultants with superscript 1 are linear functions of displacement with superscript 1. Considering this and using Eqs. (9) and Eqs. (11), the stability equations become

$$\delta u_0^1 : N_{xx,x}^1 + N_{xy,y}^1 = 0 \tag{12}$$
$$\delta v_0^1 : N_{xy,x}^1 + N_{yy,y}^1 = 0$$
$$\delta w_0^1 : M_{xx,xx}^1 + M_{yy,yy}^1 + 2M_{xy,xy}^1 + N_{xx}^0 w_{0,xx}^1 + N_{yy}^0 w_{0,yy}^1 + 2N_{xy}^0 w_{0,xy}^1 = 0$$

The stability equations in terms of the displacement components may be obtained by inserting Eqs. (10) into the above equations. Upon substitution, second and higher order terms of the incremental displacements may be omitted. Resulting equations are three stability equations based on the Kirchhoff plate theory for porous material plate.

$$A_2 u_{0,xx}^1 + C_2 u_{0,yy}^1 + (B_2 + C_2)v_{0,xy}^1 - \left(A_3 w_{0,xxx}^1 + (B_3 + 2C_3)w_{0,xyy}^1\right) = 0$$
$$(B_2 + C_2)u_{0,xy}^1 + A_2 v_{0,yy}^1 + C_2 v_{0,xx}^1 - \left(A_3 w_{0,yyy}^1 + (B_3 + 2C_3)w_{0,xxy}^1\right) = 0 \tag{13}$$
$$-\left(A_3 u_{0,xxx}^1 + (B_3 + 2C_3)u_{0,xyy}^1\right) - \left(A_3 v_{0,yyy}^1 + (B_3 + 2C_3)v_{0,xxy}^1\right)$$
$$+ \left(A_4\left(w_{0,xxxx}^1 + w_{0,yyyy}^1\right) + 2(B_4 + 2C_4)w_{0,xxyy}^1\right) + N_{xx}^0 w_{0,xx}^1$$
$$+ N_{yy}^0 w_{0,yy}^1 = 0$$

where

$$A_2, A_3, A_4 = \int_{-\frac{h}{2}}^{\frac{h}{2}} A_1(1, z, z^2)dz$$

$$B_2, B_3, B_4 = \int_{-h/2}^{h/2} B_1(1, z, z^2)dz$$

$$C_2, C_3, C_4 = \int_{-h/2}^{h/2} G(1, z, z^2) dz$$

## 4 Boundary conditions

As stated, only plates with all edges simply supported are consider in this work, Out-of-plane boundary conditions for simply supported edges are

$$
\begin{aligned}
x = 0, a: \ & w_0^1 = M_{xx}^1 = 0 \\
y = 0, b: \ & w_0^1 = M_{yy}^1 = 0
\end{aligned}
\tag{14}
$$

The in-plane boundary conditions of the simply supported edges may be of the free to move (FM) type. This is classified as follow

$$
\begin{aligned}
x = 0, a: \ & u_o^1 = finite, \ v_o^1 = finite, \quad N_{xy}^0 = 0, \quad N_{xx}^0 = -\frac{P_x}{b} \ (FM) \\
y = 0, b: \ & u_o^1 = finite, \ v_o^1 = finite, \quad N_{xy}^0 = 0, \quad N_{yy}^0 = 0 \ (FM)
\end{aligned}
\tag{15}
$$

where a bar over each parameter stands for the known external forces applied at boundaries.

## 5 Mechanical buckling analysis

The functions for displacements that satisfy the governing equations and boundary conditions are

$$
\begin{aligned}
u_o^1 &= \sum_{m=1}^{M} \sum_{n=1}^{N} u_{mn}^1 \cos(\beta x) \sin(\gamma y) \\
v_o^1 &= \sum_{m=1}^{M} \sum_{n=1}^{N} v_{mn}^1 \sin(\beta x) \cos(\gamma y) \\
w_0^1 &= \sum_{m=1}^{M} \sum_{n=1}^{N} w_{mn}^1 \sin(\beta x) \sin(\gamma y)
\end{aligned}
\tag{16}
$$

where

$$\beta = \frac{m\pi}{a}, \quad \gamma = \frac{n\pi}{b} \qquad m, n = 1,2,3,\dots$$

Substitution of Eqs. (16) into Eqs. (13) yield

$$
\begin{aligned}
K_{11} &= A_2\beta^2 + C_2\gamma^2 \\
K_{12} &= \beta\gamma(B_2 + C_2) \\
K_{13} &= -\left(A_3\beta^3 + \beta\gamma^2(B_3 + 2C_3)\right) \\
K_{22} &= A_2\gamma^2 + C_2\beta^2 \\
K_{23} &= -\left(A_3\gamma^3 + \beta^2\gamma(B_3 + 2C_3)\right) \\
K_{33} &= A_4(\beta^4 + \gamma^4) + 2\beta^2\gamma^2(B_4 + 2C_4) + N_{xx}^0\beta^2 + N_{yy}^0\gamma^2
\end{aligned}
\tag{17}
$$

For a nontrivial solution of these equations, the coefficients of functions must be set to zero. Setting $\left|K_{ij}\right| = 0$, the value of the $N_{xx}^0$ is found as

$$-N_{xx}^0 = \frac{1}{\beta^2}\left[\frac{P_1}{P_2} + A_4(\beta^4 + \gamma^4) + 2\beta^2\gamma^2(B_4 + 2C_4)\right] + N_{yy}^0\left(\frac{\gamma}{\beta}\right)^2 \tag{18}$$

where

$$P_1 = K_{11}K_{23}^2 - 2K_{12}K_{23}K_{13} + K_{22}K_{13}^2$$
$$P_2 = K_{11}K_{22} - K_{12}^2$$

By substitution ($m = 1, n = 1$), the critical mechanical load for thermo-porous-elastic plate buckling is obtained. Introducing the dimensionless form for $P_x$ as $P^* = \frac{P_x}{G_0 h^2}$ and substitution of Eqs. (15) into Eq. (18) and solving for $P^*$ yields

$$P^* = \frac{b}{G_0\beta^2 h^2}\left[\frac{P_1}{P_2} + A_4(\beta^4 + \gamma^4) + 2\beta^2\gamma^2(B_4 + 2C_4)\right] \tag{19}$$

## 6 Result and discussion

The buckling of rectangular plates made of porous material with variable properties along the thickness under uniform outside compressive load is investigated in this paper. The effects of poroelastic parameters on critical buckling load $P^*$ are investigated and presented.
Figure (2) shows the variations of shear modulus with porous distribution in thickness direction. The Biot coefficient $\left(\alpha = 1 - \frac{G(z)}{G_0}\right)$ indicates the effect of porosity on the solid constituents of poroelastic plate and it shows the effect of generated stresses in the pores on the poroelastic material in undrained condition ($\zeta = 0$). This relation shows that the Biot coefficient depends on the porosity and its distribution. By substituting Eq. (1) into the Biot relation, this coefficient is obtained as $\alpha = e_1\cos\left(\left(\frac{\pi}{2h}\right)\left(z + \frac{h}{2}\right)\right)$ at the bottom of the plate $\left(-\frac{h}{2}\right)$. It reduces across the thickness direction to zero at top of the plate. This figure shows variations of the shear modulus with porous distribution in thickness direction for the cases;
a - porous/nonlinear nonsymmetric distribution with shear modulus
$G(z) = G_0\left[1 - e_1\cos\left(\left(\frac{\pi}{2h}\right)\left(z + \frac{h}{2}\right)\right)\right]$,
b- porous/nonlinear symmetric distribution with shear modulus
$G(z) = G_0\left[1 - e_1\cos\left(\frac{\pi}{2h}\right)z\right]$,
c -porous/monotonous distribution with shear modulus
$G(z) = G_0[1 - e_1]$,
d – and homogeneous/isotropic with shear modulus $G_0$.

Figure (3) shows the effect of dimension changes on the critical buckling load of the porous/nonlinear nonsymmetric distribution plate. By increasing the length to width ratio of the plate, the critical buckling load ($P^*$) reduces. Also, by increasing the thickness of the plate, the critical buckling load ($P^*$) increases. This results are the same for all types of materials investigated in this paper, such as porous/nonlinear symmetric distribution, porous/monotonous distribution, and the homogeneous/isotropic plates, but their critical buckling loads have difference values.

Figure (4) shows the effect of thickness change on the critical buckling load for porous/ nonlinear symmetric distribution, porous/monotonous distribution, and the homogeneous/ isotropic plates. By increasing the thickness of the plate, the critical buckling load $(P^*)$ increases.

Figures (5) shows the effect of porous and thickness change on the critical buckling load for the porous/nonlinear nonsymmetric distribution plate. As seen in these figure, by increasing the thickness, the critical buckling load $(P^*)$ increases. By increasing the porosity, the free spaces within the plate increases and shear modulus decrease with respect to the first of Eqs. (1). Also, increasing the porosity of the plate decreases the critical buckling load.

In Figure (6) the effect of pores distribution on critical buckling load for the undrained condition and for simply supported edges is presented. In these figures the critical buckling load for the homogeneous case is larger than the other cases and for the case of porous/nonlinear symmetric distribution the critical buckling load is also larger than the other cases of porous plate. As the figure indicates, the plate has lowest resistance to the critical buckling load when the pores distribute symmetrically in all directions. Also it is observed that the pores distribution and $e_1$ have significant effect on the critical buckling load. By substituting $e_1 = 0, \nu_u = \nu$, Eq. (19) is reduced to the buckling load of homogeneous/isotropic plates

$$P^* = \frac{\pi^2 h}{6b(1-\nu)} \left( \frac{\left( \frac{mb}{a} \right)^2 + (n)^2}{\frac{mb}{a}} \right)^2$$

The above equation is reported by Brush and Almroth [29].

Biot [1] investigated the pore compressibility effect on critical buckling load and expressed that the critical load is proportional to the pore fluid compressibility and in drained condition the critical buckling load is the least. In porous materials the Skempton pore pressure coefficient introduces the properties of the pore fluid. The values of the undrained Poisson ratio and the Skempton pore pressure coefficient depend upon the pore fluid compressibility. The relation between Skempton coefficient and undrained Poisson ratio for saturated case is as given by the second of Eqs. (5).

If the compressibility of the pore fluid is high $(B \longrightarrow 0)$, the behavior of plate resembles that of a porous plate without fluid (drained). By setting this condition in the second of Eqs. (5), the least value of $\nu_u$ is obtained. In this case we have the least critical buckling load. When the compressibility of pore fluid is small $(B \longrightarrow 0)$, the behavior of plate resembles that of a rigid solid. Hence, with respect to the pore fluid compressibility, the Skempton coefficient changes between two values of 0 and 1, $(0 < B < 1)$.

Figures (7) and (8) show the effect of pore fluid properties on the buckling load. The effect of compressibility and porous thickness for porous/nonlinear nonsymmetric distribution plate is showed in figure (7). This figure shows that by increasing the thickness, the critical buckling load $(P^*)$ of the plate is increased. Also, by increasing the pore compressibility of the plate, the critical buckling load $(P^*)$ decreases. This results are the same for all types of materials that are investigated here, but their critical buckling loads have difference values. Figure (8) shows that the pore compressibility depend linearly on temperature and its linear function with

temperature holds for special types of fluids $B = (\frac{1}{\omega})T$. Here, $\omega$ shows different values of fluid temperature between two points. For example, for special gas this function is convenient because for $T = 0°C$ the behavior of plate resembles that of a porous plate without fluid ($B \rightarrow 0$) and for $T = 100°C$ the behavior of plate resembles that of a rigid solid, ($B \rightarrow 0$). Increasing the temperature tends to decrease the compressibility of the fluid within the pores, due to fluid trapped within the pores, where the critical buckling load is increased, except for the porous/nonlinear nonsymmetric distribution.



**Figure $(2 - a)$** Shear modulus variation associated with different coefficient of plate porosity for porous/nonlinear nonsymmetric distribution
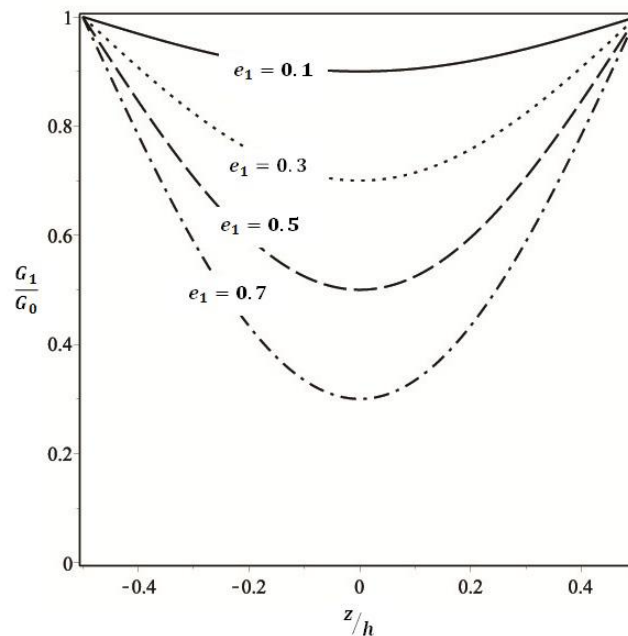


**Figure $(2 - b)$** Shear modulus variation associated with different coefficient of plate porosity for porous/nonlinear symmetric distribution
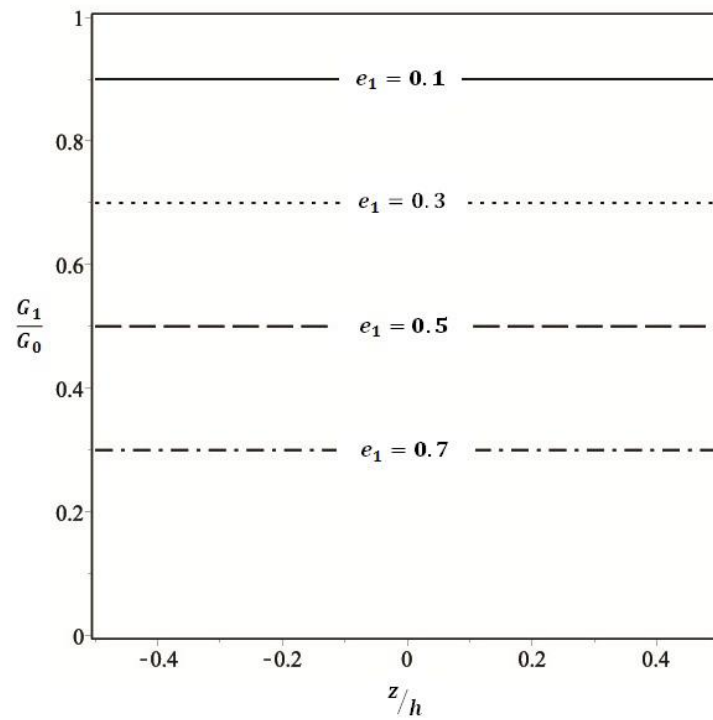
**Figure** $(2 - c)$ Shear modulus variation associated with different coefficient of plate porosity for porous/monotonous distribution
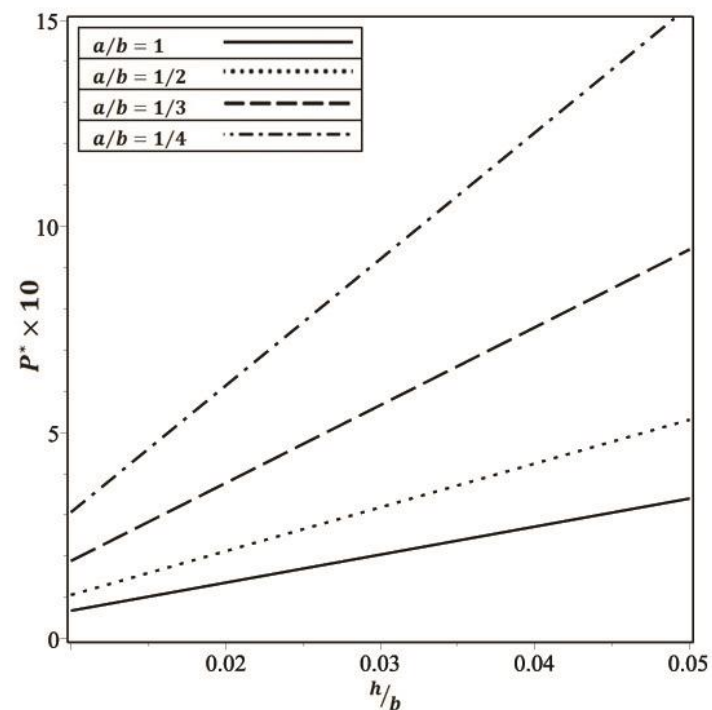


**Figure 3** Critical buckling load $(P^* \times 10)$ vs. thickness to width ratio of the porous/nonlinear nonsymmetric distribution plate, for the cases of $[a/b = 1, 1/2, 1/3, 1/4]$, $B = 0.5$, $e_1 = 0.5$ with $v = 0.3$.
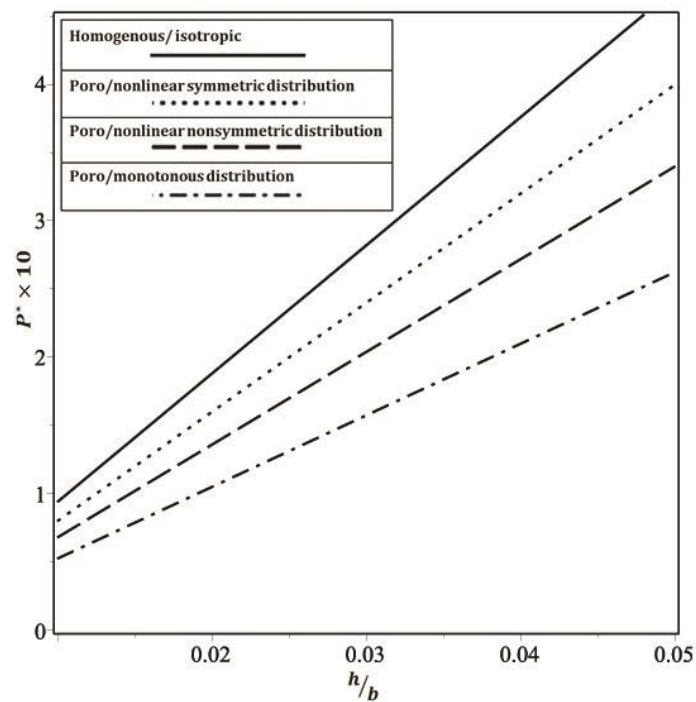
**Figure 4** Critical buckling load ($P^* \times 10$) vs. thickness to width ratio of the plate, for the cases of porous/nonlinear nonsymmetric distribution, porous/nonlinear symmetric distribution, porous/monotonous distribution, $B = 0.5$, $e_1 = 0.5$ with $a/b = 1$, $\nu = 0.3$ and homogenous/isotropic.
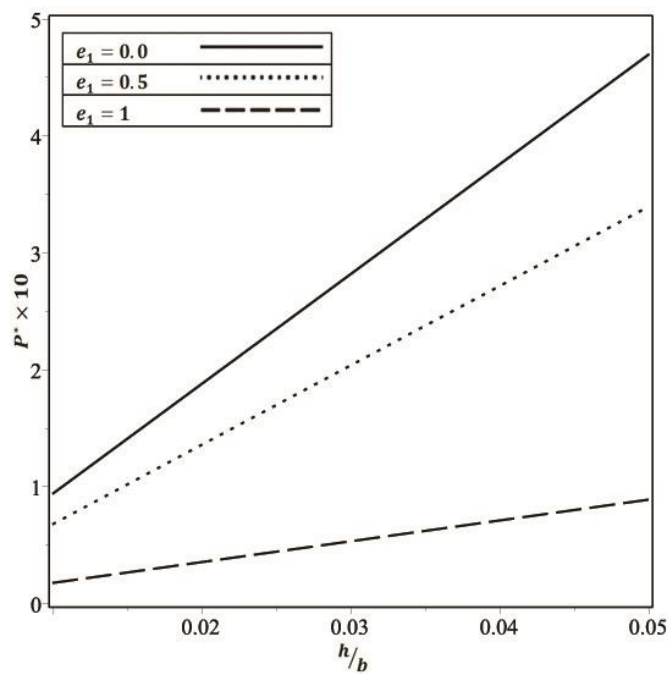


**Figure 5** Critical buckling load ($P^* \times 10$) vs. thickness to width ratio of the porous/nonlinear nonsymmetric distribution plate, for the cases of coefficient of plate porosity [$e_1 = 0.0, 0.5, 1$], $B = 0.5$, $a/b = 1$ with $\nu = 0.3$.
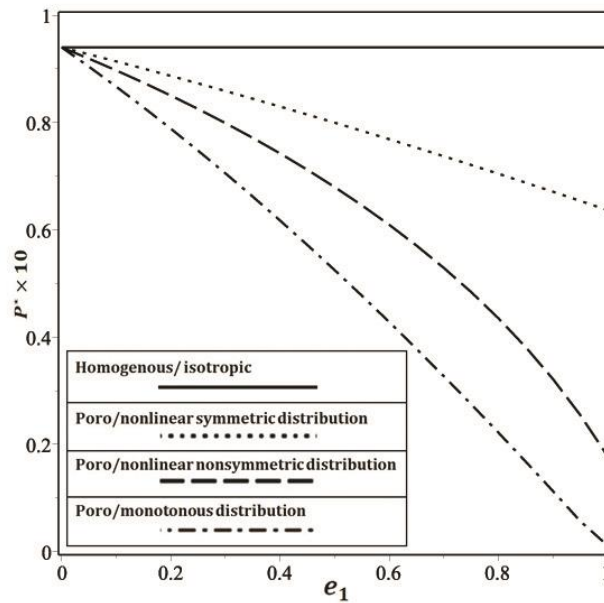
**Figure 6** Critical force ($P^* \times 10$) vs. coefficient of plate porosity, for the cases of porous/nonlinear nonsymmetric distribution, porous/nonlinear symmetric distribution, porous/monotonous distribution $B = 0.5$, with $a/b = 1$, $h/b = 0.01$, $v = 0.3$ and homogenous/isotropic
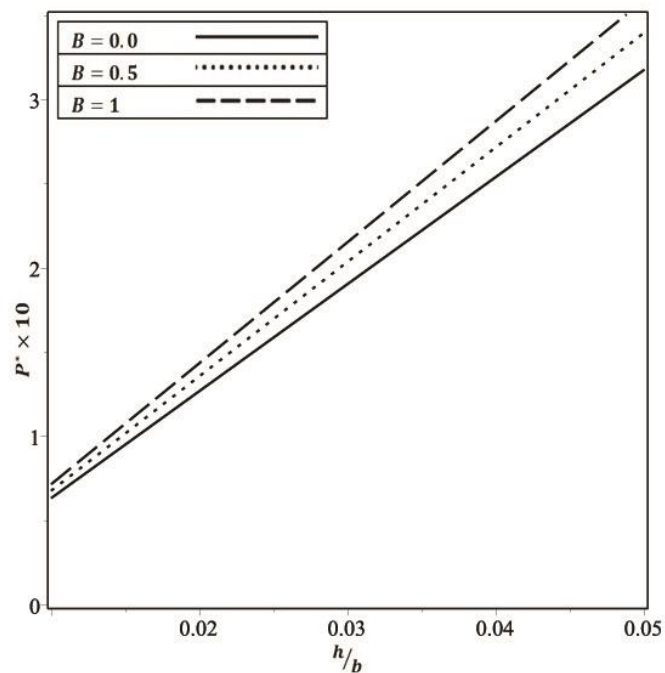


**Figure 7** Critical force ($P^* \times 10$) vs. thickness to width ratio of the porous/nonlinear nonsymmetric distribution plate, for the cases of Skempton coefficient of porous plate, $[B = 0.0, 0.5, 1]$, $e_1 = 0.5$ with $a/b = 1$, $v = 0.3$ and homogenous/isotropic
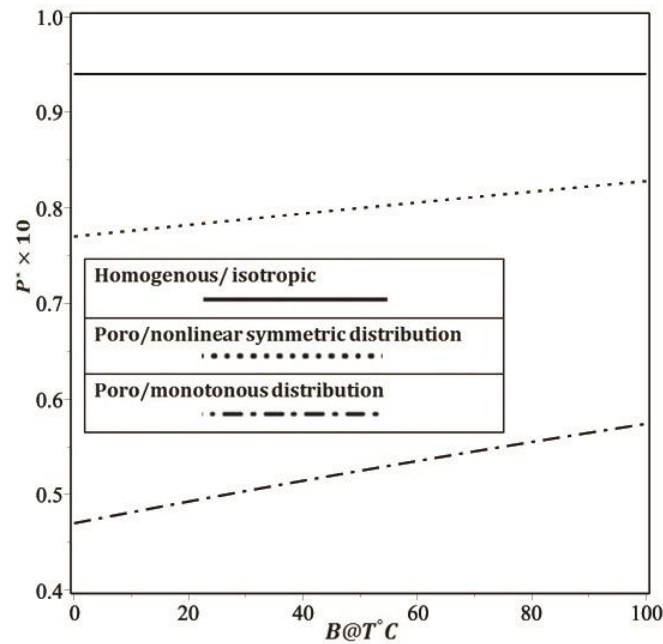
**Figure 8** Critical buckling load ($P^* \times 10$) vs. the Skempton coefficient of porous plate, for the cases of porous/nonlinear symmetric distribution, porous/monotonous distribution, $e_1 = 0.5$ with $a/b = 1$, $h/b = 0.01$, $v = 0.3$ and homogenous/isotropic

## 7 Conclusions

In the present article, the energy method is used for the buckling analysis of plate made of pore material and derivation is based on the classical plate theory with the assumption of power law composition for the constituent materials. The boundary conditions of plate are assumed to be simply supported. Two edges of the plate is subjected to uniform compressive in-plane loads. Also, effect of temperature on fluid compressibility for symmetric porous material plate is investigated. It is concluded that:

1. The buckling load ($P^*$) decreases by increasing the length along the load direction to width ratio of plate $a/b$.

2. By increasing the thickness of the plate, the buckling load ($P^*$) increases.

3. By increasing the coefficient of porosity ($e_1$) the buckling load ($P^*$) is reduced.

4. The plate behavior tends to that of the homogeneous/ isotropic behavior by reducing the porosity.

5. The monotonous porosity is lower buckling load ($P^*$) compared to the anisotropic porosity. Location of the pores in porous materials has relevant effects on the critical buckling load.

6. By increasing the Skempton coefficient, the compressibility of fluid within the pores decrease and the buckling load ($P^*$) increases.

7. By increasing the temperature, thermal expansion of fluid in the pores is more than thermal expansion of solid. Therefore the compressibility of the fluid within the pores reduced and the critical buckling load is increased.

**Acknowledgements**

**References**

[1] Biot, M.A., "Theory of Buckling of a Porous Slab and its Thermoelastic Analogy", J. Appl. Mech. ASME, Vol. 31, No. 2, pp. 194-198, (1964).

[2] Magnucki, K., and Stasiewicz, P., "Elastic Buckling of a Porous Beam", J. Theor Appl. Mech. Vol. 42, No. 4, pp. 859-868, (2004).

[3] Magnucki, K., Malinowski, M., and Kasprzak, J.," Bending and Buckling of a Rectangular Porous Plate", Steel Compos Struct, Vol. 6, No. 4, pp. 319-333, (2006).

[4] Magnucka-Blandzi, E., "Dynamic Stability of a Metal Foam Circular Plate", J. Theor Appl. Mech. Vol. 47, No. 2, pp. 421-433, (2009).

[5] Jasion, P., Magnucka-Blandzi, E., Szyc, W., and Magnucki, K., "Global and Local Buckling of Sandwich Circular and Beam-rectangular Plates with Metal Foam Core", Thin-Walled Struct, Vol. 61, pp. 154-161, (2012).

[6] Zimmerman, R.W., "Coupling in Poroelasticity and Thermoelasticity", Int. J. Rock Mech. Min Sci, Vol. 37, No. 1, pp. 79-87, (2000).

[7] Ghassemi, A., and Zhang, Q., "A Transient Fictitious Stress Boundary Element Method for Poro-thermoelastic Media", J. Eng Analysis with Boundary Elements, Vol. 28, No. 11, pp. 1363-1373, (2004).

[8] Ghassemi, A., "Stress and Pore Pressure Distribution around a Pressurized, Cooled Crack in Low Permeability Rock", Proceedings of the Thirty-Second Workshop on Geothermal Reservoir Engineering Stanford University, Stanford, California, USA, January, (2007).

[9] Jabbari, M., Mojahedin, A., Khorshidvand, A.R., and Eslami, M.R., "Buckling Analysis of Functionally Graded Thin Circular Plate made of Saturated Porous Materials", ASCE's J. Eng Mech, Vol. 140, pp. 287-295, (2013).

[10] Jabbari, M., Hashemitaheri, M., and Mojahedin, A., "Thermal Buckling Analysis of Functionally Graded Thin Circular Plate made of Saturated Porous Materials", J. Therm Stress, Vol. 37, pp. 202-220, (2014).

[11] Jabbari, M., Farzaneh Joubaneh, E., and Mojahedin, A., "Thermal Buckling Analysis of a Porous Circular Plate with Piezoelectric Actuators Based on First Order Shear Deformation Theory", Int. J. Mech Sci, Vol. 83, pp. 57-64, (2014).

[12] Farzaneh Joubaneh, E., Mojahedin, A., Khorshidvand, A.R., and Jabbari, M.," Thermal Buckling Analysis of Porous Circular Plate with Piezoelectric Sensor-actuator Layers under Uniform Thermal Load", J. Sandwich Struct Mater, Vol. 17, pp. 3-25, (2015).

[13] Mojahedin, A., Farzaneh Joubaneh, E., and Jabbari, M., "Thermal and Mechanical Stability of a Circular Porous Plate with Piezoelectric Actuators", Acta Mecanica, Vol. 83, pp. 57-64, (2014).

[14] Jabbari, M., Mojahedin, A., and Haghi, M., "Buckling Analysis of Thin Circular FG Plates Made of Saturated Porous-softferro Magnetic Materials in Transverse Magnetic Field", Thin-Walled Struct, Vol. 85, pp. 50-56, (2014).

[15] Kumar, R., Kumar, S., and Gourla, M.G., "Interaction Due to Expanding Surface Loads in Thermoporoelastic Medium", Mater Phys Mech, Vol. 21, pp. 126-134, (2014).

[16] Javaheri, R., and Eslami, M.R., "Buckling of Functionally Graded Plates under in-plane Compressive Loading", ZAMM, Vol. 82, pp. 277-283, (2002).

[17] Javaheri, R., Eslami, M.R., "Thermal Buckling of Functionally Graded Plates", AIAA J. Vol. 40, pp. 162-169, (2002).

[18] Javaheri, R., and Eslami, M.R., "Thermal Buckling of Functionally Graded Plates Based on Higher Order Theory", J. Therm. Stress, Vol. 25, No. 7, pp. 603-625, (2002).

[19] Lanhe, W., "Thermal Buckling of a Simply Supported Moderately Thick Rectangular FGM Plate", Compos Struct. Vol. 64, No. 2, pp. 211-218, (2004).

[20] Shariat, B.A.S., and Eslami, M.R., "Buckling of Thick Functionally Graded Plates under Mechanical and Thermal Loads", Compos Struct, Vol. 78, No. 3, pp. 433-439, (2007).

[21] Mohammadi, M., Saidi, A.R., and Jomehzadeh, E., "A Novel Analytical Approach for the Buckling Analysis of Moderately Thick Functionally Graded Rectangular Plates with Two Opposite Edges Simply Supported", Mech Eng Sci, Vol. 224, pp. 1831-1841, (2010).

[22] Mohammadi, M., Saidi, A.R., and Jomehzadeh, E., "Levy Solution for Buckling Analysis of Functionally Graded Rectangular Plates", Appl Compos Mater, Vol. 17, pp. 81-93, (2010).

[23] Bodaghi, M., and Saidi, A.R., "Levy-type Solution for Buckling Analysis of Thick Functionally Graded Rectangular Plates Based on the Higher-order Shear Deformation Plate Theory", Appl Math Model, Vol. 34, No. 11, pp. 3659-3673, (2010).

[24] Bodaghi, M., and Saidi, A.R., "Thermoelastic Buckling Behavior of Thick Functionally Graded Rectangular Plates", Arch Appl Mech, Vol. 81, No. 11, pp. 1555-1572, (2011).

[25] Bateni, M., Kiani, Y., and Eslami, M.R., "A Comprehensive Study on Stability of FGM Plates", Int. J. Mech Sci, Vol. 75, pp. 134-144, (2013).

[26] Behravan Rad, A., and Shariyat, M., "Three-dimensional Magneto-elastic Analysis of Asymmetric Variable Thickness Porous FGM Circular Plates with Non-uniform Tractions and Kerr Elastic Foundations", Compos Struct, Vol. 125, pp. 558-574, (2015).

[27] Swaminathan, K., Naveenkumar, D.T., Zenkour, A.M., and Carrera, E., "Stress, Vibration and Buckling Analyses of FGM Plates-A State-of-the-art Review", Compos Struct, Vol. 120, pp. 10-31, (2015).

[28] Chen, D., Yang, J., and Kitipornchai, S., "Elastic Buckling and Static Bending of Shear Deformable Functionally Graded Porous Beam", Compos Struct, Vol. 133, pp. 54–61, (2015).

[29] Chen, D., Yang, J., and Kitipornchai, S., "Free and Forced Vibrations of Shear Deformable Functionally Graded Porous Beams", Int. J. Mech Sci, Vol. 108-109, pp. 14–22, (2016).

[30] Brush, D.O., and Almroth, B.O., *"Buckling of Bars, Plates and Shells"*, McGraw-Hill, New York, USA, (1975).

[31] Wang, C.M., Reddy, J.N., and Lee, K.H., *"Shear Deformable Beams and Plates: Relationships with Classical Solutions"*, Oxford, Elsevier, (2000).

[32] Detournay, E., and Cheng, A.H.D., *"Fundamentals of Poroelasticity"*, Comprehensive Rock Engineering, Vol. 2, Pergamon Press, New York, USA, (1993).

[33] Eslami, M.R., *"Thermo-Mechanical Buckling of Composite Plates and Shells"*, Amirkabir University Press, Tehran, Iran, (2010).

**Nomenclatures**

$E$　　　　　　　　: Young's modulus of elasticity

$G$　　　　　　　　: Shear modulus of elasticity

$e_1$　　　　　　　: Coefficient of plate porosity

$\nu$　　　　　　　　: Poisson's ratio

$\varepsilon_{xx}$ , $\varepsilon_{yy}$　　　　: Normal strains

$\gamma_{xy}$ , $\gamma_{yz}$ , $\gamma_{xz}$　: Shear strains

$u, v, w$　　　　　: Displacement components in the $x$, $y$, and $z$ directions

$u_0$ , $v_0$ , $w_0$　　　: Displacement on middle plate surface

$p$　　　　　　　　: Pore fluid pressure

$\lambda_u$　　　　　　　: Lame parameters

$M$　　　　　　　　: Biot's modulus

$\zeta$　　　　　　　　: Variation of fluid volume content

$\nu_u$　　　　　　　: Undrained Poisson's ratio

$B$　　　　　　　　: Skempton coefficient

$\alpha$　　　　　　　　: Biot coefficient of effective stress

$\beta_s'$　　　　　　　: Volumetric thermal expansion coefficient of the bulk solid under constant pore pressure and stress

$\beta_s''$ , $\beta_f$　　　　: Volumetric thermal expansion coefficients of the solid matrix and the pore fluid

$\varepsilon$　　　　　　　　: Volumetric strain

## چکیده

در این تحقیق تحلیل کمانش ورق مستطیلی جامد متشکل از مواد متخلخل در شرایط آندرین بررسی شده است. خواص مکانیکی ورق در امتداد ضخامت ورق متغیر فرض شده است. توزیع تخلخل در امتداد ضخامت ورق به صورت نامتقارن غیر خطی، متقارن غیر خطی و توزیع یکنواخت در نظر گرفته شده است.

اثر تخلخل و توزیع تخلخل بر بار بحرانی کمانش ورق متخلخل مورد مطالعه قرار گرفته است. تاثیر تراکم پذیری سیال بر بار کمانش بحرانی در شرایط آندرین ارزیابی شده است. همچنین، اثر دما بر تراکم پذیری سیال در ورق پروالاستیک متقارن با انتخاب یک تابع خطی بررسی می شود. نتایج بدست آمده برای ورق های متخلخل، با داده موجود در تحقیقات پیشین تأیید شده است.